

Cite this: *J. Mater. Chem. B*, 2016,
4, 7859

Redox-mediated dissociation of PEG–polypeptide-based micelles for on-demand release of anticancer drugs

Huiyun Wen,^{*a} Haiqing Dong,^{*b} Jie Liu,^a Aijun Shen,^c Yongyong Li^b and Donglu Shi^{bd}

Intelligent nanoparticles are capable of prolonged blood circulation without leakage of the payload and fast drug release upon exposure to environmental stimuli, such as redox stimuli, and therefore are highly desirable for cancer therapy. In this study, polymeric micelles were designed and developed with a hydrophilic poly(ethylene glycol) (PEG) shell and a hydrophobic poly-L-phenylalanine (PPhe) core, linked by a redox cleavable bond, *i.e.* mPEG-SS-PPhe. The mPEG-SS-PPhe micelles were loaded with the anticancer drug doxorubicin (DOX) and shown an on-demand release profile in the presence of redox agents such as glutathione (GSH). Remarkably, the GSH-triggered micellar dissociation accelerated *in vitro* release of DOX 4.87 fold faster at 10 mM GSH than that without GSH at 12 h. An enhanced inhibitory effect of DOX-loaded mPEG-SS-PPhe micelles was achieved by improving the intracellular GSH levels. Confocal laser scanning microscopy and flow cytometric analyses of HeLa cells further confirmed that DOX accumulation was accelerated by elevating the extracellular GSH concentrations. In addition, mPEG-SS-PPhe micelles showed excellent biocompatibility on L929 and HeLa cell lines. These redox-sensitive polymeric micelles may provide more possibilities as promising carriers for on-demand drug release in a controlled manner.

Received 12th September 2016,
Accepted 3rd November 2016

DOI: 10.1039/c6tb02364a

www.rsc.org/MaterialsB

1. Introduction

Cancer nano-therapeutics have received great attention over the past few decades,^{1–4} and a broad range of polymeric nanoparticles for anticancer drug carriers has been designed and developed for clinical use, such as NK105, NK911, NC-6004, and Genexol[®]-PM.⁵ Ideally, polymeric nanocarriers should be capable of possessing three major requirements to deliver drugs to the tumor cells successfully.^{6,7} First, the nanoparticles need to be stable in the prolonged circulation of blood vessels. Second, the nanoparticles must accumulate in the tumor tissues effectively by either active or passive targeting. Third, the nanoparticles are dissociated quickly to achieve intracellular drug release locally in the tumor cells. A variety of nanocarriers, including polymeric micelles,^{8,9} liposomes,^{10,11} prodrugs,^{12,13} and nanogels,^{14,15} have been developed to fulfill these requirements.

Polymeric micelles are a fascinating class of nanocarriers with well-defined core–shell nanostructures, which commonly assembled by amphiphilic copolymers with distinct hydrophobic and hydrophilic segments.¹⁶ In addition, their small sizes are attractive for passive targeting in tumor sites through the leaky vasculature *via* a unique enhanced permeation and retention (EPR) effect.¹⁷ Poly(ethylene glycol) (PEG) is the most commonly used hydrophilic block segment due to its high hydrophilicity, biocompatibility, and electrical charge neutrality for non-immunogenicity.^{18,19} It is noteworthy that micelles with PEG shells are often referred to as “stealthy” nanoparticles, because they possess a prolonged circulation time and reduced uptake by the macrophages of the reticuloendothelial system (RES).²⁰ However, it is reported that PEG shells also suppress the cellular uptake of micelles by the tumor cells.^{21,22} Shedding of the PEG shell remains an important issue for drug release from polymeric micelles.²³ The above issues on maintaining prolonged blood circulation and intracellular drug release can be addressed by employing stimuli responsiveness to micelles.²⁴ Wang and coworkers developed an acid-sensitive micellar nanoparticle (PEG-Dlinkm-R9-PCL) that exhibited superior gene silencing efficiency and tumor inhibition activity.²⁵ During blood circulation, the acid-sensitive bridged copolymer remained stable due to PEG corona induced protection from RES clearance. At pH 6.5, however, the breakage of acid linkage induced PEG detachment and exposed the cell-penetration

^a School of Chemical Engineering, Northwest University, Xi'an, P. R. China.
E-mail: huiyunwen@mwu.edu.cn

^b The Institute for Translational Nanomedicine, Shanghai East Hospital, The Institute for Biomedical Engineering & Nano Science (iNANO) Tongji University School of Medicine, Shanghai, P. R. China.
E-mail: inano_donghq@tongji.edu.cn

^c Department of Medical Imaging, Nantong Tumor Hospital, Nantong University, Nantong, P. R. China

^d The Materials Science and Engineering Program, Department of Mechanical and Materials Engineering, College of Engineering and Applied Science, University of Cincinnati, Cincinnati, 45221, USA

peptide (R9) thus leading to increased cell uptake and siRNA delivery.

Although remarkable progress with PEG detachable release has been achieved using various stimuli triggers, research on redox-sensitive disulfide linked shedding strategies continues to be a very active field. The disulfide bond can be cleaved by reducing agents such as glutathione (GSH).^{26,27} It is reported that the intracellular GSH level (2–10 mM) is 1000-fold higher than that in the blood plasma (2–20 μM).²⁸ In particular, some tumor cells typically exhibit elevated cytosolic GSH levels compared to that in normal cells.^{29,30} Therefore, it is interesting to develop redox-sensitive nanoparticles for controlling the shedding of PEG shells. A number of redox-sensitive conjugates have been developed for successful PEG detachment and subsequent fast release of anti-cancer drugs in the presence of redox agents.³¹ Recently, Zhong and co-workers reported PEG-based micelles (cRGD20/PEG-SS-PCL) as drug delivery carriers.³² Their results showed that the disulfide bonds in DOX-loaded cRGD20/PEG-SS-PCL micelles were stable in blood circulation with an elimination half-life time of 3.51 h. However, the disulfide bonds in micelles were cleaved in 10 mM GSH followed by accelerated drug release as compared to cRGD/PEG-PCL micelles without disulfide bonds. Similarly, the synthesized OCT(Phe)-PEG-ss-PTX prodrug micelles were stable during blood circulation, but quickly dissociated at the 20 mM GSH level followed by rapid release of PTX into the cytoplasm.³³

The hydrophobic segments in reported redox sensitive micelles are, however, subject to some limitations, such as the complicated PEGylation strategy and, most importantly, the lack of biocompatibility. Unlike the conventional hydrophobic segments such as poly(lactic-co-glycolic acid) (PLGA) and poly(lactic acid) (PLA), polypeptides upon degradation do not produce acidic products but naturally occurring amino acids.^{5,34} Typically, polypeptides are usually synthesized by ring-opening polymerization (ROP) of α -amino acid *N*-carboxyanhydrides (NCAs).^{35,36} They have several advantages including excellent biocompatibility, biodegradability,

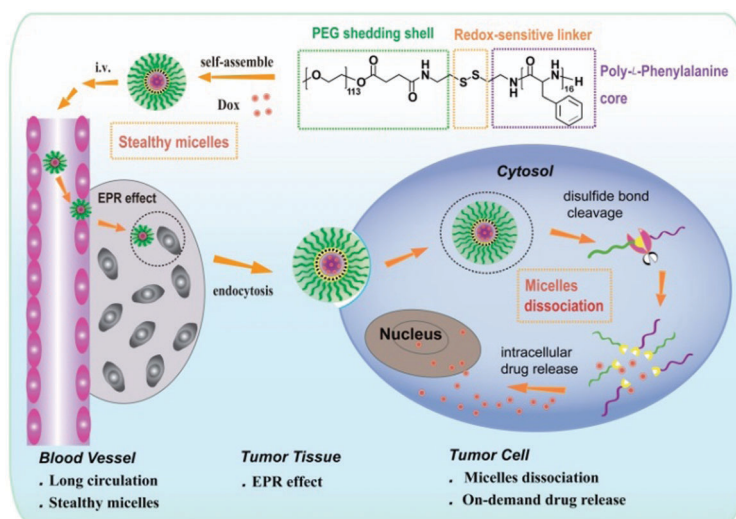
non-antigenicity, and easy functionality. Kataoka and co-workers performed an extensive research study on various PEG-poly-(amino acids) micelles.^{37,38} The most popular amino acids in the hydrophobic core of micelles include lysine, aspartic acid, and histidine.³⁹ Nevertheless, unlike lysine which requires further hydrophobic modification,⁴⁰ phenylalanine is a natural amino acid with hydrophobic benzyl groups that can be used directly as hydrophobic segments. Furthermore, the π - π interaction between benzyl groups is favorable for the structural stabilization of micelles with high affinity to aromatic anti-cancer drugs. Despite all these merits, phenylalanine-based polypeptides are still not well-utilized as building blocks of redox micelles for controlled drug delivery.

Herein, we developed in this work a redox sensitive micelle based on the amphiphilic copolymer poly(ethylene glycol)-*block*-poly-L-phenylalanine (mPEG-SS-PPhe) with a disulfide linkage. These PEG-polypeptide-based micelles can load the hydrophobic anticancer drug doxorubicin (DOX) by physical entrapment. As illustrated in Scheme 1, in the presence of blood-relevant GSH, the micelles are maintained with prolonged circulation. However, the disulfide linkages are expected to be cleaved in the presence of tumor cytosolic-relevant GSH once the DOX-loaded micelles are endocytosed into tumor cells. Thus the detachment of PEG shells results in micelle dissociation and rapid intracellular release of encapsulated cargos. In this study, we introduced a new class of peptide-based redox sensitive micelles for on-demand anti-cancer drug delivery.

2. Experimental section

2.1 Materials and methods

Poly(ethylene glycol) monomethyl ether ($\text{CH}_3\text{O-PEG}$, $M_n \approx 5000 \text{ g mol}^{-1}$, GL Biochem, Ltd), fluorescein isothiocyanate (FITC, Acros), and triethylamine (Et_3N , 99%, Sigma) were used as received. L-Phenylalanine (99%), triphosgene (99%),



Scheme 1 Predicted GSH mediated mPEG-SS-PPhe micelle dissociation for on-demand release of DOX.

cystamine dihydrochloride (98%), *N*-hydroxysuccinimide (NHS, 98%), 1-ethyl-3-(3-dimethylaminopropyl) carbodiimide hydrochloride (EDC·HCl, 98.5%), glutathione (GSH, 98%), 4-dimethylamino-pyridine (DMAP, 99%) and succinic anhydride (A.R.) were purchased from Aladdin chemistry Co. Ltd and used as received. Doxorubicin hydrochloride (DOX·HCl, Aladrich) was desalinated before use. Tetrahydrofuran (THF, Shanghai Chemical Reagent Co. Ltd) and 1,4-dioxane (Shanghai Chemical Reagent Co. Ltd) were dried over CaH₂ for 24 h at room temperature (r.t.) and distilled before use. *N,N*-Dimethyl formamide (DMF, Shanghai Chemical Reagent Co. Ltd) were dried over CaH₂ for 24 h at r.t. and distilled under vacuum conditions before use. Dulbecco's modified Eagle's medium (DMEM), penicillin–streptomycin, fetal bovine serum (FBS), dubelcco's phosphate buffered saline (DPBS) and trypsin were obtained from Gibco Invitrogen Corp. 4% paraformaldehyde was purchased from Dingguo Changsheng Biotech. Co., Ltd. The WST-1 cell proliferation and cytotoxicity assay kit was purchased from Beyotime Institute of Biotechnology.

2.2 Synthesis of mPEG-COOH

The solution of mPEG (2 g, 0.4 mmol) and DMAP (0.05 g, 0.4 mmol) was dissolved in 40 mL of anhydrous 1,4-dioxane under a nitrogen atmosphere at r.t. Succinic anhydride (0.1 g, 1 mmol) was added for further reaction of 24 h. Afterwards, the solution was concentrated using the rotary evaporation method. The obtained mixture was subsequently dispersed in 20 mL of saturated sodium chloride aqueous solution. Upon removal of the white precipitate by filtration, the product dissolved in aqueous solution was extracted with dichloromethane (DCM, CH₂Cl₂, 3 × 20 mL) three times. The combined organic layer was concentrated by rotary evaporation and precipitated in cold ethyl ether three times. The white solids (mPEG-COOH) were dried under vacuum at 30 °C. Yield: 86%.

2.3 Synthesis of mPEG-SS-NH₂

First, cystamine dihydrochloride was pretreated with NaOH solution through acid–base neutralization. Briefly, the solution of cystamine dihydrochloride (0.17 g, 1.1 mmol) was dissolved in 20 mL of aqueous solution stirred at r.t. and NaOH (88 mg, 2.2 mmol) was dissolved in 10 mL of aqueous solution was added dropwise. After 30 min, the aqueous solvent was removed under vacuum conditions. Then the solution was diluted with 30 mL of dichloromethane. The insoluble salts in DCM (CH₂Cl₂) were removed by filtration. Cystamine was obtained after removing DCM by rotary evaporation.

Second, mPEG-SS-NH₂ was prepared by mPEG-COOH and cystamine through amidation reaction. Briefly, mPEG-COOH (1 g, 0.2 mmol), NHS (0.23 mmol) and EDC·HCl (0.62 mmol) were dissolved in 30 mL of anhydrous CH₂Cl₂ and stirred under a nitrogen atmosphere at r.t. for 5 h. Cystamine (0.15 g, 1 mmol) was then added dropwise for further reaction of 24 h. The resulting solution was concentrated by rotary evaporation and precipitated in cold ethyl ether three times. The white solids (mPEG-SS-NH₂) were dried under vacuum at 30 °C. Yield: 79%.

2.4 Synthesis of L-phenylalanine *N*-carboxyanhydride (Phe-NCA)

Synthesis of L-phenylalanine *N*-carboxyanhydride (Phe-NCA) was accomplished according to the Fuchs–Farthing method.⁴¹ Briefly, L-phenylalanine (1 g, 6 mmol) was suspended in anhydrous tetrahydrofuran (THF, 30 mL) at 70 °C. Under a nitrogen atmosphere, triphosgene (0.74 g, 2.5 mmol) in 20 mL of anhydrous THF was subsequently added dropwise to the solution. The further reaction time of 4 h was allowed until the solution became clear. Then the mixture was concentrated at 25 °C under vacuum. The desired intermediate Phe-NCA was subsequently purified by precipitation in *n*-hexane twice. The white solids (Phe-NCA) were dried under vacuum at 30 °C. Yield: 72%.

2.5 Synthesis of GSH-cleavable block copolymers (mPEG-SS-PPhe)

mPEG-SS-PPhe block copolymers were prepared by ring-opening polymerization (ROP) of Phe-NCA using amino-terminated PEG (mPEG-SS-NH₂) as an initiator. Briefly, Phe-NCA (0.25 g, 1.27 mmol) and mPEG-SS-NH₂ (0.5 g, 0.1 mmol) were added in anhydrous dimethylformamide (DMF, 10 mL) under a nitrogen atmosphere for further reaction time of 48 h at r.t. The mPEG-SS-PPhe copolymers were purified by dialyzing against deionized (DI) water (molecular weight cut-off, MWCO: 10–12 kDa) for 48 h and subsequently freeze-dried for further use. Yield: 84%.

2.6 Synthesis of FITC-labeled mPEG-SS-PPhe copolymers

Fluorescein isothiocyanate (FITC) was used to label mPEG-SS-PPhe copolymers for fluorescence microscopy evaluation.⁴² Briefly, in the presence of triethylamine (Et₃N), FITC (50 mg) was added to a solution of mPEG-SS-PPhe (50 mg) in anhydrous DMF (5 mL) and stirred for 48 h. The mPEG-SS-PPhe–FITC conjugates were purified by dialyzing against DI water (MWCO: 10–12 kDa) for 48 h and subsequently freeze-dried for further use.

2.7 Characterization methods

Fourier transform infrared (FTIR) spectra of samples were recorded on a Tensor 27 FTIR spectrometer (Bruker, Germany). Proton nuclear magnetic resonance (¹H NMR) spectra of samples were obtained using an Avance 500 MHz spectrometer (Bruker bioSpin, Switzerland) with DMSO-*d*₆ or D₂O as solvent. Tetramethylsilane (TMS) was used as a standard. Gel permeation chromatography (GPC) analysis was conducted on a gel permeation chromatographic system equipped with a waters 150C separation module and a Waters differential refractometer, using THF as an eluent at a flow rate of 1 mL min⁻¹. The molecular weight and its distributions were calibrated against polystyrene standards. The morphology of micelles was investigated by using a Hitachi H7100 transmission electron microscope (TEM, Hitachi, Ltd, Hong Kong) at an acceleration voltage of 100 kV. Briefly, 10 μL of the micelle suspension was dropped on copper grids and stained with phosphotungstic acid. The morphology was observed after the samples were

dried. The hydrodynamic radius (R_h) of micellar aggregates was determined by the dynamic light scattering spectrophotometry method (DLS) using a Nano-ZS 90 Nanosizer (Malvern Instruments Ltd, Worcestershire, UK).

2.8 Self-assembly behavior

Micelles of the mPEG-SS-PPhe copolymer in PBS were prepared by the dialysis method at r.t. Briefly, the copolymer dissolved in DMF (0.8 mg mL^{-1}) was dialyzed (MWCO 10–12 kDa) against DI water (2 L) for 24 h. The DI water was changed every 6 h.

The critical micelle concentration (CMC) of the copolymer was measured on a fluorescence spectrometer (F-2500, Hitachi, Ltd, Hongkong) using pyrene as a fluorescence probe.⁴³ Briefly, 100 μL of a pyrene solution in acetone ($\sim 6 \mu\text{M}$) was added to a test tube. When acetone was evaporated, 2 mL of an aqueous solution of mPEG-SS-PPhe ranging from $1.2 \times 10^{-3} \text{ mg mL}^{-1}$ to 0.5 mg mL^{-1} was added to the test tube separately. After sonication for 5 min, the mixture was kept at r.t. for 24 h to allow pyrene equilibrating in the aqueous phase. Fluorescence spectra were recorded on a Hitachi F-2500 luminescence spectrometer with an excitation wavelength of 330 nm. The emission wavelengths were recorded ranging from 350 nm to 500 nm. The CMC value was estimated as the cross-point of intensity of I_{397} to the micelle concentration.

2.9 Preparation of DOX-loaded micelles

DOX was encapsulated into mPEG-SS-PPhe micelles by the dialysis method.⁴⁴ 0.8 mg of DOX-HCl was first desalinated in the presence of 20 μL Et_3N to obtain DOX. DOX was then added to a solution of mPEG-SS-PPhe (8 mg) in 10 mL of DMF under moderate stirring for 4 h. Finally, DOX-loaded micelles were prepared by dialysis (MWCO 10–12 kDa) against DI water for 24 h. The dialysis medium was changed every 6 h.

The fluorescence intensity of free DOX without loading in the micelles (DOX WOL-micelles) was determined by fluorescence spectrophotometry (Em: 470 nm, Ex: 559 nm). The amount of DOX WOL-micelles was obtained using a standard curve, $C \text{ (mg mL}^{-1}\text{)} = I/156.32$. The amount of DOX encapsulated in the micelles was calculated by subtracting the amount of DOX-WOL micelles from the initial feeding amount.⁴⁴ The drug loading content (DLC) and drug loading efficiency (DLE) of DOX were calculated using eqn (1) and (2), respectively.

$$\text{DLC}(\%) = \frac{\text{Amount of DOX loaded in micelles}}{\text{Total amount of micelles}} \times 100 \quad (1)$$

$$\text{DLC}(\%) = \frac{\text{Amount of DOX loaded in micelles}}{\text{Initial feeding amount of DOX}} \times 100 \quad (2)$$

2.10 Structural stability of micelles in the GSH environment

The stability of micelles in response to GSH trigger was adapted from the literature.⁴⁵ Typically, 10 mM GSH was added to the prepared micelles and kept at 37 °C. The size distribution of micelles was measured by DLS at 0 h, 0.5 h, 1 h, 2 h, and 24 h, respectively.

2.11 GSH-mediated *in vitro* DOX release

The *in vitro* release behavior of DOX was studied in PBS release medium (pH 7.4) with various GSH concentrations (0, 2 μM and 10 mM), which was placed in a shaking bed (150 rpm) at 37 °C.⁴⁵ At predetermined time points, 2 mL of release medium was taken out and subsequently replenished with 2 mL of fresh PBS. Then the amount of DOX released from the micelles was calculated by fluorescence spectrophotometry (excitation: 470 nm, emission: 559 nm).

The cumulative amount of DOX released from micelles was calculated using eqn (3).

$$\text{Cumulative DOX release}(\%) = \frac{M_t}{M_0} \times 100 \quad (3)$$

where M_t is the total amount of DOX released from micelles at time t , and M_0 is the amount of DOX initially loaded into the micelles.

2.12 Cell lines

Cancer cell lines (the human epitheloid cervix carcinoma, HeLa) and normal cell lines (L929) were both supplied by the Cell Center of Tumor Hospital at Fudan University (Shanghai, China). Cells were propagated in T-75 flasks under an atmosphere of 5% CO_2 at 37 °C and grown in DMEM supplemented with 10% fetal bovine serum and 0.1% penicillin–streptomycin.

2.13 *In vitro* cytotoxicity and antitumor effects of DOX-loaded micelles

Using a standard WST-1 assay, the *in vitro* cytotoxicity of DOX-free micelles and DOX loaded micelles were evaluated against L929 cells and HeLa cells. In brief, cells were seeded in 96-well plates at a density of 5000 cells per well in 200 μL DMEM medium and subsequently incubated under a 5% CO_2 atmosphere at 37 °C. After incubation for 24 h, 200 μL samples of DOX-free micelles or DOX loaded micelles with different concentrations (31.3×10^{-3} – 1 mg mL^{-1}) were added to the cells for an additional 24 h incubation. The WST-1 solution (10 μL) and 100 μL of fresh DMEM medium were then added to the cells. After 2 h incubation, the absorbance (ABS) of each well was measured at 450 nm using a microplate reader (Bio-Rad, Thermo fisher scientific, Waltham, MA, USA). Cell viability was calculated using eqn (4).^{44,46}

$$\text{Cell viability}(\%) = \frac{\text{ABS}_{\text{sample treated cells}} - \text{ABS}_{\text{free medium}}}{\text{ABS}_{\text{control untreated cells}} - \text{ABS}_{\text{free medium}}} \times 100 \quad (4)$$

Data were presented as average (SD (n 5)).

2.14 Time-dependent cellular uptake of drug-free micelles

To observe time-dependent cellular uptake of drug-free micelles, FITC was conjugated to the mPEG-SS-PPhe copolymers.⁴² HeLa cells were seeded into a 6-well plate at a density of 1×10^5 cells per well for 24 h incubation. 0.5 mg mL^{-1} FITC-labeled mPEG-SS-PPhe copolymers were subsequently added to the cells at incubation times of 30 min, 1 h, 2 h, and 4 h, respectively. The cells were washed with DPBS twice and observed by fluorescence microscopy

(Niko Eclipse 80i) at an excitation wavelength of 495 nm and an emission wavelength of 500–590 nm. The images were utilized for both qualitative and quantitative analysis.

To quantitatively analyze the fluorescence intensity (I) of micelle uptake by cells, a white line was drawn across each image.⁴⁷ The total fluorescence intensities distributed on the white line were obtained through computational profile analysis using Image J software. The integral of fluorescence intensity curve along the white line indicated the amount of micelles taken up by HeLa cells, which was calculated using eqn (5):

$$I = \int_0^d f(x) dx \quad (5)$$

where I is the integral of fluorescence intensity along the line; d is the length of the white line, and $f(x)$ is the function of fluorescence intensity corresponding to the location on the white line, which can be detected using Image J.

2.15 Intracellular DOX release

Intracellular DOX release behavior was observed by laser scanning confocal microscopy (LSCM, Leica TCS SP5 II, Germany) and flow cytometry assessment (BD Biosciences, USA).⁴⁸ HeLa cells were incubated in microscope slides at a density of 1×10^5 cells in 2 mL of culture medium. After 24 h incubation, FITC-modified DOX-loaded micelles (0.5 mg mL^{-1}) were added to the cells for an additional 4 h incubation. The cells were rinsed three times with DPBS. 4% paraformaldehyde was added and kept at r.t. for 15 min. The cells were rinsed three times again with DPBS. The cells were observed by CLSM with excitation wavelengths of 488 nm (red) and 495 nm (green), respectively.

For the flow cytometry assessment, HeLa cells were seeded onto a six-well plate at a density of 1×10^5 cells per well in 2 mL of DMEM and incubated for 24 h. Cells were pre-treated with 10 mM GSH for 2 h using non-pretreated cells as the control. The cells were rinsed three times with DPBS (pH 7.4), and incubated with DOX-loaded micelles (0.25 mg mL^{-1}) for 2 h in DMEM. In the next step, the cells were trypsinized and centrifuged at 1000 rpm for 5 min, then collected and rinsed three times with DPBS (pH 7.4) containing 2% (v/v) FBS and 2 mM EDTA. Finally the cells were suspended in paraformaldehyde solution (500 μL , 2%) for flow cytometry analyses.

2.16 Statistical analysis

In vitro cell proliferation assay was performed in 5 replicate wells. Mean and standard deviation were tabulated. Student's *t*-test was used to determine statistical difference among groups at a significance level $p < 0.05$. Data are presented as mean \pm SD.

3. Results and discussion

3.1 Synthesis and characterization of copolymers

Successful conjugation of the biocompatible building blocks PEG and the poly-L-phenylalanine polypeptide was achieved *via* disulfide bonds to develop mPEG-SS-PPhe copolymers. The synthesis

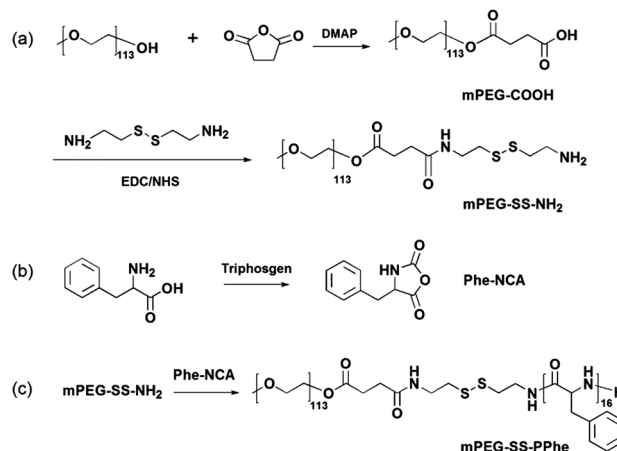


Fig. 1 Synthesis route of disulfide-linked mPEG-SS-PPhe copolymers.

route of mPEG-SS-PPhe is shown in Fig. 1. Efficient polymerization of Phe-NCA was accomplished by the ring-opening polymerization (ROP) mechanism using amino PEG with a disulfide bond (mPEG-SS-NH₂) as an initiator. The mPEG-SS-NH₂ to Phe-NCA ratio was kept at 2 : 1 (w/w). Because of the polypeptide core being linked to PEG by disulfide bonds, the block copolymer would be cleaved under redox conditions.

FTIR spectra of mPEG-SS-PPhe and its key intermediates mPEG-COOH and mPEG-SS-NH₂ are shown in Fig. 2. After amide reaction, the characteristic peak at 1633 cm^{-1} corresponds to the absorption of the amide carbonyl group (O=CNH). The peak at 1526 cm^{-1} is characteristic of the absorption of –N–H– in PPhe units. These FTIR spectra indicate successful ROP reaction leading to the formation of mPEG-SS-PPhe copolymers using mPEG-SS-NH₂ as an initiator.

The ¹H NMR spectra of mPEG-COOH and Phe-NCA are presented in Fig. 3(a) and (b), respectively. δ 3.50 and δ 7.2 ppm attributed to the characteristic signals of mPEG and PPhe-NCA, respectively. Moreover, evaluation of a representative ¹H NMR spectrum of mPEG-SS-PPhe copolymers (Fig. 3(c)) shows characteristic chemical shifts for hydrogens at both the mPEG moiety ($\delta = 3.51 \text{ ppm}$) and the PPhe fragment

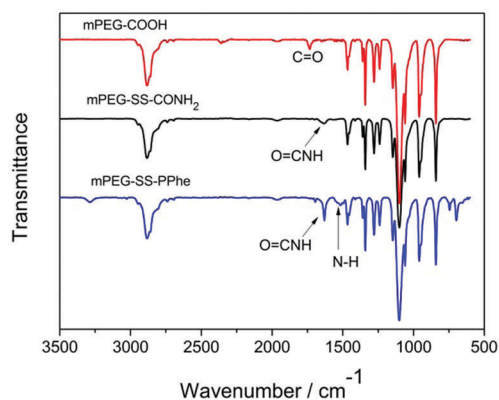


Fig. 2 FTIR spectra of mPEG-SS-PPhe copolymers and their key intermediates mPEG-COOH, mPEG-SS-NH₂.

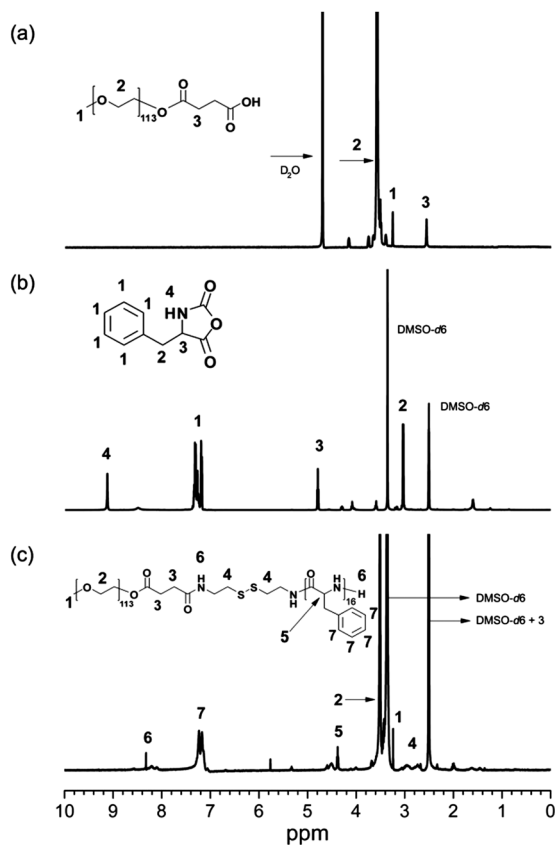


Fig. 3 ^1H NMR spectrum of mPEG-COOH in D_2O , Phe-NCA and mPEG-SS-PPhe in $\text{DMSO}-d_6$.

($\delta = 4.4$ and 7.23 ppm), respectively. The molecular weight (M_n NMR) of mPEG-SS-PPhe was 7900 g mol^{-1} calculated by the ^1H NMR analysis. This result indicated that the copolymers contained an average of 16 Phe residues (*i.e.*, mPEG-SS-PPhe₁₆).

Fig. 4 shows the GPC traces of mPEG-SS-PPhe copolymers. The GPC curve of mPEG-SS-PPhe copolymers exhibits a narrow PDI value and shifts towards a higher molecular weight compared with mPEG. As shown in Fig. 4, the molecular weight (M_n GPC) of mPEG-SS-PPhe, determined by GPC, is 8100 g mol^{-1} , which agrees with the result of the ^1H NMR analysis.

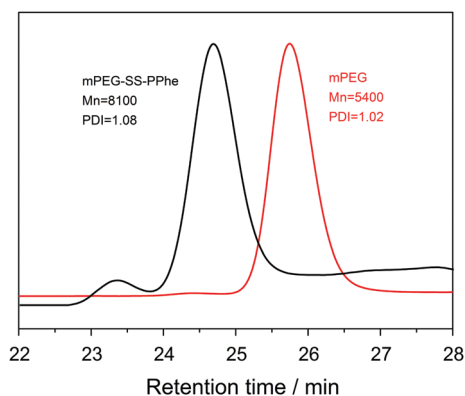


Fig. 4 GPC traces of mPEG and mPEG-SS-PPhe copolymers in THF.

3.2 Preparation and characterization of micelles

The mPEG-SS-PPhe self-assembled micelles were prepared *via* the dialysis method. The particle size, morphology, and CMC value were analyzed. DLS shows that the hydrodynamic diameter of micelles is approximately 210 nm with a relatively narrow PDI of 0.15 (Fig. 5a). However, the TEM image displays a smaller size with a homogeneous spherical outline of micelles (Fig. 5b). The relatively small size observed by TEM is due to the volume shrinkage of micellar samples caused by water loss, whereas DLS measures the hydrodynamic diameter (micelle + bound water) of the micellar aggregates. Nevertheless, both characterization methods indicate the successful formation of micellar assemblies.

To underline the amphiphilic behavior of synthesized copolymers, the critical micelle concentration (CMC) of copolymers was experimentally measured using a fluorescence spectrometer with pyrene as a fluorescence probe (Fig. 5c). The CMC value of mPEG-SS-PPhe micelles was estimated to be 38 mg L^{-1} (Fig. 5d). ^1H NMR spectroscopy detected in D_2O further confirmed the formation of micellar assemblies. As shown in Fig. 5d, chemical shifts at $\delta 3.56$ attribute to the characteristic signals of mPEG. Unlike the spectrum detected in $\text{DMSO}-d_6$ (Fig. 3c), the characteristic signals from the PPhe segment ($\delta 7.2$) disappeared in D_2O . These results show the shielding of the hydrophobic PPhe core by a hydrophilic PEG shell in D_2O solvent, suggesting the successful formation of micellar structures.

3.3 The structural dissociation of micelles in response to GSH conditions

It is known that GSH responsive copolymers with redox-cleavable linkages can be designed to have two functions: the stability in a physiological environment and dissociation in a redox environment.

We investigated the structural dissociation behavior of mPEG-SS-PPhe micelles by DLS measurements^{40,45} in the presence of biological reducing agents, such as GSH. As shown in Fig. 6a, GSH-induced size growth of mPEG-SS-PPhe micelles is investigated in 10 mM GSH at pH 7.4 over a period of 24 h by DLS. In the presence of 10 mM GSH, the micelle size increased quickly from 210 nm to 400 nm after 0.5 h. This is because of the partial detachment of PEG shells from micelles induced by the cleavage of disulfide bonds. Formation of larger aggregates (>1000 nm, corresponding to a newly formed minor signal peak) was even more pronounced after 2 h. This is attributed to the cleavage of the disulfide bonds between the hydrophilic PEG shell and the hydrophobic PPhe core in the presence of 10 mM GSH. Thus, the abundant detachment of PEG shells destroyed the balance of the micellar structure, causing micelle dissociation and thermodynamic aggregation of polypeptide segments. In contrast, no obvious change in micelle size was observed over 24 h in the absence of GSH. Zhong and coworkers have reported similar results that the size of micelles increased from 85 nm to 110 nm in 10 mM GSH after 10 h.⁴⁹ Compared with their results, our micelles had a higher sensitivity to

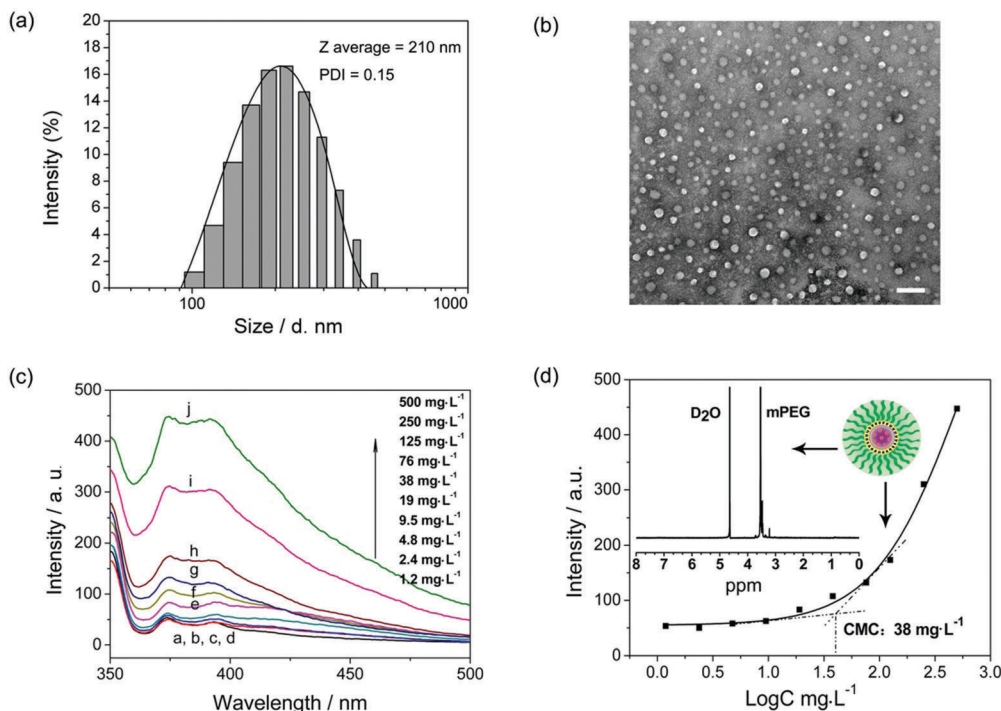


Fig. 5 (a) Representative size distribution of mPEG-SS-PPhe micelles (0.8 mg mL^{-1} in PBS) determined by DLS; (b) TEM images of mPEG-SS-PPhe micelles, scale bar = 200 nm; (c) CMC fluorescence emission spectra of pyrene with mPEG-SS-PPhe micelles, excitation wavelength: 330 nm; (d) CMC value and ^1H NMR spectra of mPEG-SS-PPhe micelles in D_2O (inset).

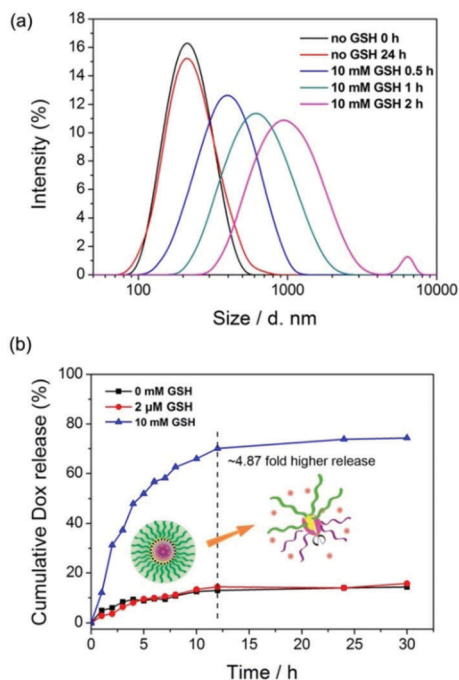


Fig. 6 (a) Time-dependent changes in mPEG-SS-PPhe micelle size upon exposure to 10 mM GSH as determined by DLS; (b) GSH-sensitive drug release from DOX-loaded mPEG-SS-PPhe micelles in PBS.

the GSH levels. The GSH-induced dissociation of micelles is expected to achieve the on-demand intracellular release of the loaded drug.

3.4 *In vitro* GSH triggered on-demand release behavior of DOX

To experimentally assess GSH-induced *in vitro* drug release from micelles, the cytotoxic anticancer drug doxorubicin (DOX) was encapsulated into mPEG-SS-PPhe micelles by a solvent change method. The DOX loading content (DLC) and DOX loading efficiency (DLE) of micelles were 6.52% and 65.2%, respectively.

To experimentally explore the effect of GSH levels on *in vitro* DOX release, micelles loaded with DOX were performed in three different PBS solutions at pH 7.4 with 0 mM GSH, 2 μM GSH and 10 mM GSH, respectively. Fig. 6b shows the cumulative release profiles of DOX from the prepared micelles at various GSH levels. The results showed that DOX release from micelles at 2 μM GSH (mimicking extracellular GSH levels, *i.e.* plasma)²⁸ was largely inhibited. Only less than 15% of DOX was released over 30 h. Analogous results were observed for DOX release in the absence of GSH. Notably, at the 10 mM GSH level, which is analogous to intracellular GSH concentrations in tumor cells (*i.e.* cytosol, cell nucleus),²⁸ the DOX release was remarkably enhanced in the first two hours (31.3% release of DOX). 70% of DOX was released in 12 h with approximately 4.87-fold higher than that in the absence of GSH. About 80% of drugs released after 30 h in a 10 mM GSH environment while other 20% of drug probably exhibited sustained release behavior as time increased. The reasonable explanation is due to the micelle dissociation and aggregation in the presence of GSH conditions. The rest of the drugs were wrapped in the hydrophobic aggregates and released slowly. However, we are more

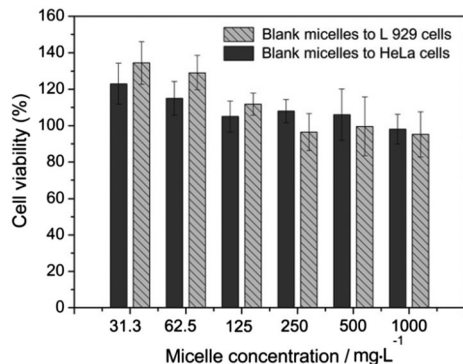


Fig. 7 Cell viability of L929 and HeLa cells incubated with mPEG-SS-PPhe micelles alone after 24 h. Data are presented as mean \pm SD ($n = 5$).

interested in the fast release behavior of the loaded drug sensitive to redox levels. This *in vitro* DOX release behavior was consistent with the rapid size change of micelles in 10 mM GSH. In addition, data from this *in vitro* release behavior suggested the GSH-induced cleavage of disulfide linkages between the PEG shell and the polypeptide core, subsequently causing the disassembly of micelles. It can be concluded, therefore, that the mPEG-SS-PPhe micelles not only are capable of loading DOX effectively but also have high sensitivity to tumor-relevant GSH levels, which remarkably accelerates DOX release. This unique GSH-dependent drug release carrier is particularly attractive for on-demand drug release in tumor cells.

3.5 *In vitro* cytotoxicity and cellular uptake of blank micelles

In vitro cytotoxicity of blank micelles was tested on both normal cells (L929 cells) and cancer cells (HeLa cells) by WST-1 assay, respectively. As shown in Fig. 7, the cell viability of blank mPEG-SS-PPhe micelles incubated with both L929 cells and HeLa cells are basically non-toxic (cell survival $>90\%$) up to a tested micelle concentration of 1 mg mL^{-1} , suggesting that blank micelles possess favorable biocompatibility.

In addition, the cellular uptake behavior of FITC-labeled micelles was monitored by fluorescence microscopy when incubated

with HeLa cells. As shown in Fig. 8a, FITC fluorescence intensifies from 30 min to 4 h, suggesting successful cell endocytosis of micelles in a time-dependent fashion. To quantitatively analyze the fluorescence intensity of micellar uptake by cells, a white line was drawn across each image.⁴⁷ The total fluorescence intensities distributed on the white line were obtained through computational profile analysis using Image J software (Fig. 8b). The average fluorescence intensity along the white line was increased from 20 to 73 as time increased from 30 min to 4 h, which further proved the time dependable uptake behavior of micelles by HeLa cells.

3.6 *In vitro* antitumor activity

The *in vitro* antitumor activity of DOX-loaded mPEG-SS-PPhe micelles was tested on HeLa cells by WST-1 assays. It is shown that encapsulation of DOX into mPEG-SS-PPhe micelles has effectively inhibited cell proliferation in a dose-dependent fashion (Fig. 9a).

The survival ratio of HeLa cells was reduced to only 25% after 24 h incubation with 0.25 mg mL^{-1} DOX-loaded micelles, which is equivalent to $16.2 \text{ } \mu\text{g mL}^{-1}$ DOX in micelles. In addition, the IC_{50} (inhibitory concentration to produce 50% cell death) value of drug-loaded micelles was estimated to be $5.496 \text{ } \mu\text{g DOX equiv. per mL}$, which was lower than those reported DOX formulations ($10.4 \text{ } \mu\text{g mL}^{-1}$,⁵⁰ and $10\text{--}60 \text{ } \mu\text{g mL}^{-1}$).⁴⁶ The high anti-tumor activity of DOX-loaded micelles indicated that DOX has been efficiently released into the nuclei of HeLa cells.

The shedding of PEG shells in 10 mM GSH led to rapid micellar disassembly, followed by enhancement of drug release and cellular uptake. To investigate the effect of GSH-triggered drug release on tumor cell viability, HeLa cells were incubated at different times with DOX-loaded micelles in the presence or absence of 10 mM GSH respectively (Fig. 9b). Notably, in the presence of 10 mM GSH, proliferation of HeLa cells was well inhibited, especially after incubation for 12 h.

3.7 Redox-induced intracellular DOX release and flow cytometric analysis

CLSM is another clear evidence for observing fast cellular uptake of DOX-loaded FITC-labeled micelles and DOX release

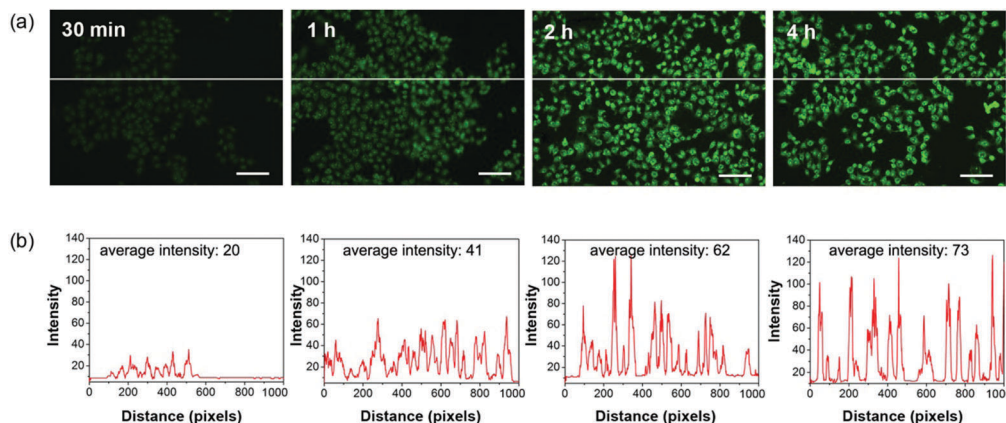


Fig. 8 (a) Time dependent cellular uptake of FITC-labeled mPEG-SS-PPhe micelles, excitation wavelength: 495 nm; scale bar = 100 μm . (b) Distributions and corresponding fluorescence intensity profiles along the white line across the images of group a, respectively.

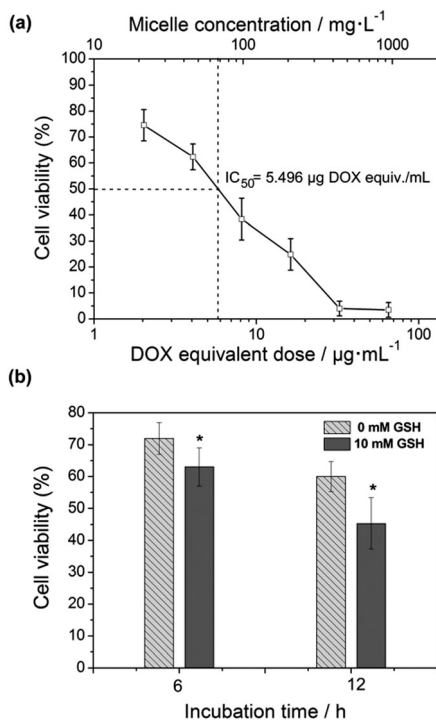


Fig. 9 (a) Cell proliferation of HeLa cells after 24 h incubation with DOX loaded mPEG-SS-PPhe micelles. Data are presented as mean \pm SD ($n = 5$); (b) cell proliferation of HeLa cells after 6 h and 12 h incubation with DOX-loaded mPEG-SS-PPhe micelles (0.5 mg mL^{-1}) in the presence of 0 mM and 10 mM extracellular GSH.

behavior. As shown in Fig. 10, red fluorescence from DOX distributes in both the cytoplasm and the nucleus of HeLa cells after 4 h incubation, especially in the nucleus of HeLa cells with pre-treated 10 mM GSH (Fig. 10b).

Thus, CLSM of HeLa cells, incubated with DOX-loaded micelles, further confirmed the DOX accumulation being accelerated

by enhanced extracellular GSH concentration. It has been reported that DOX could interact with DNA by intercalation and inhibition of macromolecular biosynthesis.⁵¹ Therefore, it is critical to release DOX intracellularly for efficient anti-tumor therapy.

Flow cytometric analyses further shows a significant DOX fluorescence difference between HeLa cells with 0 and 10 mM GSH pretreatment. Briefly, HeLa cells were pre-treated with 10 mM GSH for 2 h using non-pretreated HeLa cells (0 mM GSH) as the control. The cells were incubated with DOX-loaded micelles (0.25 mg mL^{-1}) for an additional 2 h. As shown in Fig. 11, the increased GSH levels (e.g. 10 mM) lead to stronger DOX fluorescence in HeLa cells.

Consistent with GSH-triggered *in vitro* release of DOX, the DOX-loaded mPEG-SS-PPhe micelles successfully inhibited cell proliferation in a GSH dependent manner. These results

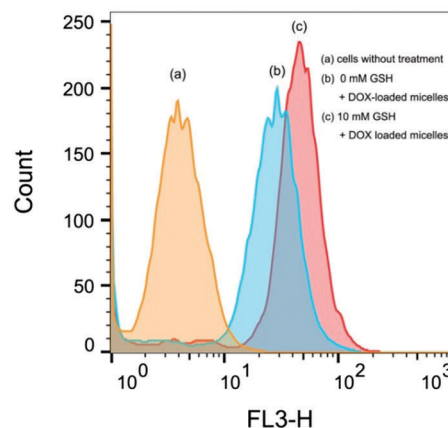


Fig. 11 Flow cytometric analyses of 0 mM and 10 mM GSH pre-treated HeLa cells incubated with DOX-loaded micelles (0.25 mg mL^{-1}) for 2 h. The equivalent Dox dose was $16.25 \mu\text{g mL}^{-1}$. HeLa cells without any treatment were used as control. Fluorescence intensity is denoted as FL3-H.

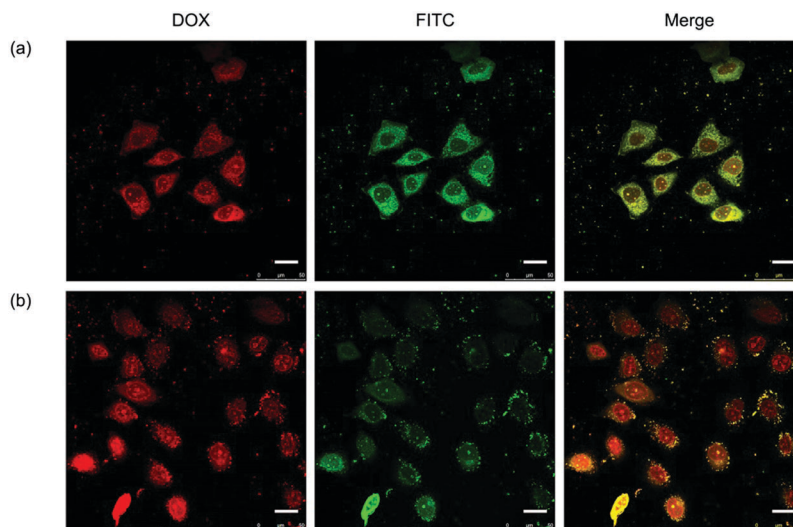


Fig. 10 Representative CLSM micrographs of HeLa cells incubated with DOX-loaded FITC-labeled micelles for 4 h in the presence of (a) 0 mM extracellular GSH and (b) 10 mM extracellular GSH concentration, respectively. (Green channel shows the fluorescence of FITC-labeled micelles, whereas the red channel visualizes DOX fluorescence.) Scale bar = 25 μm .

confirmed that mPEG-SS-PPhe micelles can release DOX intracellularly in a GSH dependent fashion.

4. Conclusion

In conclusion, redox responsive mPEG-SS-PPhe micelles have been successfully synthesized as ideal on-demand anticancer drug release carriers. The micelles are able to load DOX and exhibit GSH-responsive structure disassembly associated with highly efficient DOX release at elevated GSH levels resulting in high antitumor activity. Cell cytotoxicity assays performed on the HeLa cells indicate high antitumor activity due to DOX released from micelles. CLSM and flow cytometric analyses confirm that the DOX-loaded micelles can internalize HeLa cells quickly and demonstrated a GSH dependent intracellular DOX release behavior.

These redox sensitive, PEG-polypeptide-based micelles have the following unique merits: (i) the GSH sensitive mPEG-SS-PPhe copolymers can be easily synthesized by the ROP mechanism using amino PEG as an initiator; (ii) they possess excellent biocompatibility associated with the biocompatible PEG shell and polypeptide core, and (iii) they are responsible for both prolonged blood circulation and GSH triggered on-demand drug release. These GSH sensitive, PEG-polypeptide-based micelles are highly promising drug carriers for intracellular delivery of anti-cancer drugs.

Acknowledgements

We gratefully acknowledge financial support from the National Natural Science Foundation of China (21306152, 51473124, 31571018), the Fundamental Research Funds for the Central Universities (1500219085), the Foundation of Shaanxi Provincial Natural Science Basic Research Plan (2014JQ2067), the Foundation of Shaanxi Provincial Education Department (14JK1744) and the Nantong Science Foundation of China (MS12015100).

Notes and references

- 1 D. Peer, J. M. Karp, S. Hong, O. C. Farokhzad, R. Margalit and R. Langer, *Nat. Nanotechnol.*, 2007, **2**, 751–760.
- 2 E.-K. Lim, T. Kim, S. Paik, S. Haam, Y.-M. Huh and K. Lee, *Chem. Rev.*, 2015, **115**, 327–394.
- 3 M. Elsbahy and K. L. Wooley, *Chem. Soc. Rev.*, 2012, **41**, 2545–2561.
- 4 H. Wei, R. X. Zhuo and X. Z. Zhang, *Prog. Polym. Sci.*, 2013, **38**, 503–535.
- 5 S. Biswas, P. Kumari, P. M. Lakhani and B. Ghosh, *Eur. J. Pharm. Sci.*, 2016, **83**, 184–202.
- 6 A. Wicki, D. Witzigmann, V. Balasubramanian and J. Huwyler, *J. Controlled Release*, 2015, **200**, 138–157.
- 7 E. Blanco, H. Shen and M. Ferrari, *Nat. Biotechnol.*, 2015, **33**, 941–951.
- 8 L. Y. Tang, Y. C. Wang, Y. Li, J. Z. Du and J. Wang, *Bioconjugate Chem.*, 2009, **20**, 1095–1099.
- 9 J. M. W. Chan, J. P. K. Tan, A. C. Engler, X. Y. Ke, S. J. Gao, C. A. Yang, H. Sardon, Y. Y. Yang and J. L. Hedrick, *Macromolecules*, 2016, **49**, 2013–2021.
- 10 X. L. Liang, J. Gao, L. D. Jiang, J. W. Luo, L. J. Jing, X. D. Li, Y. S. Jin and Z. F. Dai, *ACS Nano*, 2015, **9**, 1280–1293.
- 11 N. Tripathy, R. Ahmad, H. A. Ko, G. Khang and Y. B. Hahn, *Nanoscale*, 2015, **7**, 4088–4096.
- 12 Z. X. Zhou, J. B. Tang, Q. H. Sun, W. J. Murdoch and Y. Q. Shen, *J. Mater. Chem. B*, 2015, **3**, 7594–7603.
- 13 Y. N. Zhong, K. Goltsche, L. Cheng, F. Xie, F. H. Meng, C. Deng, Z. Y. Zhong and R. Haag, *Biomaterials*, 2016, **84**, 250–261.
- 14 J. K. Oh, D. J. Siegwart, H. I. Lee, G. Sherwood, L. Peteanu, J. O. Hollinger, K. Kataoka and K. Matyjaszewski, *J. Am. Chem. Soc.*, 2007, **129**, 5939–5945.
- 15 M. Oishi, H. Hayashi, I. D. Michihiro and Y. Nagasaki, *J. Mater. Chem.*, 2007, **17**, 3720–3725.
- 16 K. Kataoka, A. Harada and Y. Nagasaki, *Adv. Drug Delivery Rev.*, 2012, **64**, 37–48.
- 17 H. Maeda, J. Wu, T. Sawa, Y. Matsumura and K. Hori, *J. Controlled Release*, 2000, **65**, 271–284.
- 18 J. S. Suk, Q. G. Xu, N. Kim, J. Hanes and L. M. Ensign, *Adv. Drug Delivery Rev.*, 2016, **99**, 28–51.
- 19 S. Schottler, G. Becker, S. Winzen, T. Steinbach, K. Mohr, K. Landfester, V. Mailander and F. R. Wurm, *Nat. Nanotechnol.*, 2016, **11**, 372–377.
- 20 R. Gref, M. Luck, P. Quellec, M. Marchand, E. Dellacherie, S. Harnisch, T. Blunk and R. H. Muller, *Colloids Surf., B*, 2000, **18**, 301–313.
- 21 S. D. Li and L. Huang, *J. Controlled Release*, 2010, **145**, 178–181.
- 22 H. Hatakeyama, H. Akita and H. Harashima, *Adv. Drug Delivery Rev.*, 2011, **63**, 152–160.
- 23 B. Romberg, W. E. Hennink and G. Storm, *Pharm. Res.*, 2008, **25**, 55–71.
- 24 H. L. Che and J. C. M. van Hest, *J. Mater. Chem. B*, 2016, **4**, 4632–4647.
- 25 C. Y. Sun, S. Shen, C. F. Xu, H. J. Li, Y. Liu, Z. T. Cao, X. Z. Yang, J. X. Xia and J. Wang, *J. Am. Chem. Soc.*, 2015, **137**, 15217–15224.
- 26 B. Deng, P. Ma and Y. Xie, *Nanoscale*, 2015, **7**, 12773–12795.
- 27 J. M. Yang, Y. C. Duan, X. Z. Zhang, Y. J. Wang and A. Yu, *J. Mater. Chem. B*, 2016, **4**, 3868–3873.
- 28 R. Cheng, F. H. Meng, C. Deng, H. A. Klok and Z. Y. Zhong, *Biomaterials*, 2013, **34**, 3647–3657.
- 29 J. Wu, L. L. Zhao, X. D. Xu, N. Bertrand, W. I. Choi, B. Yameen, J. J. Shi, V. Shah, M. Mulvale, J. L. MacLean and O. C. Farokhzad, *Angew. Chem., Int. Ed.*, 2015, **54**, 9218–9223.
- 30 A. Albin and M. B. Sporn, *Nat. Rev. Cancer*, 2007, **7**, 139–147.
- 31 L. Jia, D. Cui, J. Bignon, A. Di Cicco, J. Wdzieczak-Bakala, J. M. Liu and M. H. Li, *Biomacromolecules*, 2014, **15**, 2206–2217.
- 32 Y. Q. Zhu, J. Zhang, F. H. Meng, C. Deng, R. Cheng, F. J. Jan and Z. Y. Zhong, *J. Controlled Release*, 2016, **233**, 29–38.

- 33 T. J. Yin, Q. Wu, L. Wang, L. F. Yin, J. P. Zhou and M. R. Huo, *Mol. Pharmaceutics*, 2015, **12**, 3020–3031.
- 34 Y. Y. Guo, B. N. Niu, Q. L. Song, Y. D. Zhao, Y. L. Bao, S. W. Tan, L. Q. Si and Z. P. Zhang, *J. Mater. Chem. B*, 2016, **4**, 2338–2350.
- 35 T. J. Deming, *Adv. Mater.*, 1997, **9**, 299–311.
- 36 T. J. Deming, in *Peptide Hybrid Polymers*, ed. H. A. Klok and H. Schlaad, 2006, vol. 202, pp. 1–18.
- 37 Y. Kakizawa and K. Kataoka, *Langmuir*, 2002, **18**, 4539–4543.
- 38 Y. Kakizawa, S. Furukawa and K. Kataoka, *J. Controlled Release*, 2004, **97**, 345–356.
- 39 Y. Bae and K. Kataoka, *Adv. Drug Delivery Rev.*, 2009, **61**, 768–784.
- 40 H. Y. Wen, H. Q. Dong, W. J. Xie, Y. Y. Li, K. Wang, G. M. Pauletti and D. L. Shi, *Chem. Commun.*, 2011, **47**, 3550–3552.
- 41 A. N. Koo, H. J. Lee, S. E. Kim, J. H. Chang, C. Park, C. Kim, J. H. Park and S. C. Lee, *Chem. Commun.*, 2008, 6570–6572.
- 42 Y. N. Zhao, B. G. Trewyn, I. I. Slowing and V. S. Y. Lin, *J. Am. Chem. Soc.*, 2009, **131**, 8398–8400.
- 43 Y. Y. Li, H. Cheng, Z. G. Zhang, C. Wang, J. L. Zhu, Y. Liang, K. L. Zhang, S. X. Cheng, X. Z. Zhang and R. X. Zhuo, *ACS Nano*, 2008, **2**, 125–133.
- 44 E. S. Gil, L. F. Wu, L. C. Xu and T. L. Lowe, *Biomacromolecules*, 2012, **13**, 3533–3541.
- 45 H. L. Sun, B. N. Guo, R. Cheng, F. H. Meng, H. Y. Liu and Z. Y. Zhong, *Biomaterials*, 2009, **30**, 6358–6366.
- 46 D. Y. Cho, H. Cho, K. Kwon, M. Yu, E. Lee, K. M. Huh, D. H. Lee and H. C. Kang, *Adv. Funct. Mater.*, 2015, **25**, 5479–5491.
- 47 J. N. Zheng, H. G. Xie, W. T. Yu, M. Q. Tan, F. Q. Gong, X. D. Liu, F. Wang, G. J. Lv, W. F. Liu, G. S. Zheng, Y. Yang, W. Y. Xie and X. J. Ma, *Langmuir*, 2012, **28**, 13261–13273.
- 48 H. Y. Wen, C. Y. Dong, H. Q. Dong, A. J. Shen, W. J. Xia, X. J. Cai, Y. Y. Song, X. Q. Li, Y. Y. Li and D. L. Shi, *Small*, 2012, **8**, 760–769.
- 49 X. X. Wang, J. Zhang, R. Cheng, F. H. Meng, C. Deng and Z. Y. Zhong, *Biomacromolecules*, 2016, **17**, 882–890.
- 50 C. Wei, Y. Zhang, H. Xu, Y. Xu, Y. Xu and M. Lang, *J. Mater. Chem. B*, 2016, **4**, 5059–5067.
- 51 D. A. Gewirtz, *Biochem. Pharmacol.*, 1999, **57**, 727–741.